STABLE TRANSMISSION OF RF SIGNALS ON OPTICAL FIBER LINKS[*]

Russell Wilcox, J. M. Byrd[†], Lawrence Doolittle, Gang Huang, J. W. Staples

Lawrence Berkeley National Laboratory, One Cyclotron Road, Berkeley, California 94720, USA

Abstract

We demonstrate distribution of a 2850 MHz radio frequency signal over stabilized optical fiber links. For a 2.2 km link we measure an RMS drift of 19.4 fs over 60 hours and for a 200 m link an RMS drift of 8.4 fs over 20 hours. RF signals are transmitted as amplitude modulation on a continuous optical carrier. Variations in the delay length are sensed using heterodyne interferometry and used to correct the RF phase. The system uses standard fiber telecommunications components.
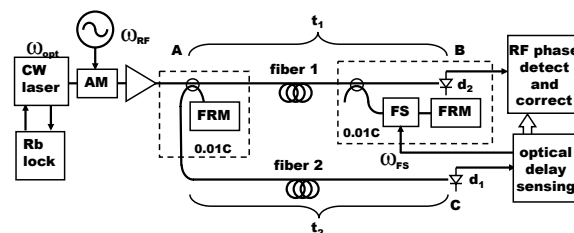
Figure 1: Schematic layout of a single channel RF transmission over an optical link. RF frequency is 2850 MHz. AM: Amplitude modulator; FRM: Faraday rotator mirror; FS: optical frequency shifter. Dotted rectangles indicate components temperature controlled to ± 0.01 C.

INTRODUCTION

The next generation of accelerator-driven light sources will produce sub-100 fs high brightness x-ray pulses[1]. Pump-probe experiments at these facilities require synchronization of pulsed lasers and RF accelerating fields on sub-100 fs time scales over distances of a few hundred meters to several kilometers. Several approaches have been implemented to send stable signals over fiber optics, with average uncertainties of a few hundred femtoseconds to under 10 fs[2, 3, 4, 5, 6].

We describe a system for stable radio frequency distribution which has demonstrated less than 20 fs RMS jitter and drift over 2.2 km of optical fiber for 60 hours, and less than 10 fs over a 200 m fiber, using common fiber telecommunications components and microwave electronics[7]. The system is easily manufacturable and low cost. It is straightforward to expand to many channels, because all delay control is done electronically in the receiver rather than by mechanical delays at the transmitter. Eliminating commonly-used mechanical delays also improves reliability and provides an arbitrarily large delay correction range, limited only by software. Because delay sensing is done using a continuous optical carrier, rapid delay changes beyond the control bandwidth are tracked continuously without jumping fringes. Standard fiber is used, requiring no dispersion compensation. Signal processing in the receiver is done digitally, so all key parameters are inherently controllable. Any frequency or combination of frequencies can be transmitted, in contrast to a fixed set of harmonics available in pulsed schemes.

RF TRANSMISSION ON STABILIZED LINKS

A schematic diagram of a single-channel RF transmission and delay stabilization link is shown in Fig. 1. In our scheme, the optical phase delay through a fiber is precisely measured using a heterodyne interferometer. This measurement is used to correct the phase error of an RF signal which is transmitted on that fiber. We can derive simplified equations for propagation of optical and RF signals through the link, assuming that the small and constant delays within the temperature controlled boxes are zero. To understand the operation of the interferometer, consider an optical wave starting at A and propagating through fiber 1 with delay t_1. At B, it is shifted in frequency by ω_{FS} by the optical frequency shifter (FS), retroreflected by the Faraday rotator mirror (FRM) and shifted in frequency again. It goes back through fiber 1 with delay t_1 to A, through a directional coupler, and through fiber 2 with delay t_2 to C. This is the "long" path. A second path through the interferometer is from A to the Faraday rotator mirror in the box at A, back through the directional coupler, and through fiber 2 to C. This is the "short" path. These two waves can be represented by their electric fields at C, which contain information as to the phase shifts each has encountered along its path. The fields can be expressed as

$$
\begin{aligned}
E_{long} &= \cos(\omega_{op}(t - t_1 - t_1 - t_2) \\
&\quad + 2(\omega_{FS}(t - t_1 - t_2) + \phi_{FS})) \quad (1) \\
E_{short} &= \cos(\omega_{op}(t - t_2)) \quad (2)
\end{aligned}
$$

where ω_{op} is the optical frequency ($2\pi 200 THz$), ω_{FS} is the frequency shifter RF frequency($2\pi 50 MHz$), and ϕ_{FS} is a phase that can be added to ω_{FS} for control. Calculating the intensity incident on detector d_1 at C, low pass filtering the AC component to remove ω_{op}, and mixing the resultant

RF with a local oscillator at $2\omega_{FS}$ yields the phase of the detected RF:

$$\phi_{det} = -2\omega_{op}t_1 - 2\omega_{FS}(t_1 + t_2) + 2\phi_{FS} \quad (3)$$

Note that $2\omega_{FS}$ is 2×10^6 smaller than ω_{op}, so the second term is negligible. If we can adjust ϕ_{FS} so that ϕ_{det} is held constant, ϕ_{FS} will directly indicate changes in t_1, given ω_{op} held constant also (as explained below). Thus we can determine changes in the optical phase delay in fiber 1, t_1, to high precision since it is measured optically.

A control loop holds ϕ_{det} constant, and the information from ϕ_{FS} is used to correct the phase of RF received on diode d_2. The phase of the output RF from the link at ω_{RF} is given by

$$\phi_{RF\_out}(t) = \omega_{RF}t - \omega_{RF}t_1 + \frac{\omega_{RF}}{\omega_{op}}\phi_{FS} \cdot k_{group\_phase}. \quad (4)$$

The first two factors on the right side are the detected RF, while the third is the correction. Ideally, the phase ϕ_{RF_out} would be just $\omega_{RF}t$, as it is at the transmitter. The additional changes due to $\omega_{RF}t_1$ are cancelled by controlling ϕ_{FS}. There is a factor k_{group_phase} which has to be included, to correct for the difference between group delay (of the RF) and phase delay (of the carrier) through the fiber due to chromatic dispersion. Chromatic dispersion in the fiber shifts the phase of the AM sidebands compared to their original phase with respect to the carrier at the modulator. This results in a slippage of modulated RF phase with respect to the optical carrier phase as the signal travels, and a difference in group delay. In practice, we measure this factor in a loop-back experiment where two channels are compared, then add it to the single-channel control software.

The operation of the interferometric optical phase control provides constant optical frequency and phase at the receiver, which has been the goal of previous transmission systems using a frequency shifter[8]. Our scheme differs from [8] in that phase sensing and frequency control is done at the receiver, making multiple channels easier to implement.

The stability of our optical phase controller was verified by constructing a Mach-Zehnder interferometer out of two such heterodyne interferometers. One 2km fiber was exposed to ambient temperature variation and and a short 2m fiber was in a temperature controlled environment. Diurnal temperature variations caused up to 2ns delay changes in the 2km fiber. After correction, the overall differential phase error between two stabilized links was six optical waves peak-to-peak over ten days[9].

For stable RF transmission, the CW laser used in the interferometer must have a fractional frequency stability less than the desired fractional temporal stability of the transmission delay. For a 2 km link with 10 fs stability, this corresponds to $\Delta\lambda/\lambda = 1 \times 10^{-9}$. The CW laser frequency is locked to a hyperfine absorption line in Rb vapor, achieving 5×10^{-10} when two independent lasers are beat together [10, 11].

A 2850 MHz RF signal is amplitude modulated onto the optical carrier by a lithium niobate modulator. The bias point is stabilized by detecting the second harmonic of the 2850 MHz modulation in a phase-locked loop. Amplitude modulation depth is typically 70%, detected by a photodiode.

One issue with photodiode detection is AM-to-PM conversion, where changes in the average optical power modulate the phase of the detected RF signal. This is usually explained as a variation in junction capacitance due to changes in peak carrier density. In our photodiodes (Discovery Semiconductor DSC50) we observe a non-monotonic AM-to-PM response, in contrast to the monotonic response found in[12]. The optical power level is set to a local maximum in the AM-to-PM photodiode response, where there is zero slope and minimal sensitivity to fluctuations in optical power. At this peak, a $\pm 10\%$ variation in average photocurrent causes less than 10 fs delay variation in the detected RF signal.

RF PHASE DETECTOR

The receiver is a digital RF phase comparator used to compare the transmitted RF signal with a local signal to be controlled. Since the delay through coax cables and other RF components is temperature dependent, variations are corrected by subtracting a local calibration signal sent through both comparison paths. Critical RF and optical components are temperature stabilized to $\pm 0.01C$.
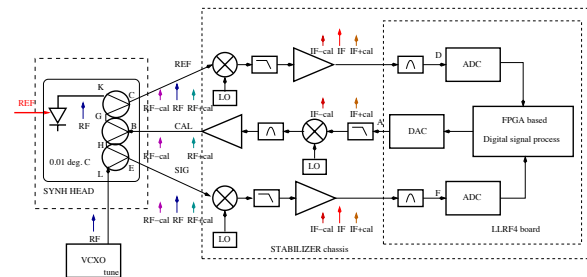

Figure 2: Schematic for phase detection.

A schematic of the signal paths in the receiver is shown in Fig. 2. The RF signal phase is measured by downconverting the RF signal, digitizing, and processing by a FPGA based signal processor. A CW double sideband suppress carrier signal (with 1.25 MHz sidebands) is added onto the RF signal as a common mode among both channels as a calibration signal. Signal paths not included in the calibration path must be temperature stabilized. The calibration signal is split to the signal and reference inputs, allowing calibration of the complete signal path through the downconversion and upconversion stages. After the signal is digitized, we measure the phase of each spectrum line in the signal and calculate the corrected RF phase accordingly. Significant care has been taken to minimize the effect of intermodulation products by using high IP3 components using the lowest possible signal power to the mixer.

An example of the phase signal before and after correction is shown in Fig. 3. Without the phase calibration correction, the effect of the lab two-hour temperature cycle is apparent. With the phase calibration correction, the residual RMS phase noise is 0.015 deg in a 125 kHz bandwidth. Note that the effective phase noise depends on the bandwidth response of the remote client to be synchronized.
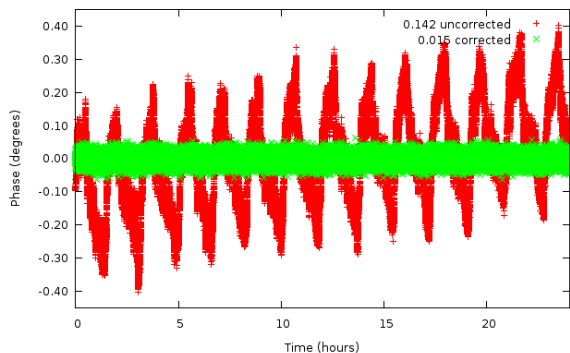

Figure 3: Out of loop measurement of the relative phase with and without calibration correction. The two hour period variation is due to lab temperature cycling. With calibration, the RMS phase noise is 0.015 deg at 2856 MHz in a 125 kHz bandwidth.

RESULTS

Measured relative time difference between long and short stabilized links are shown in Fig. 4 for a 2.2 km and for a 200 m fiber in one of the two channels, and 2 m in the other. There is a 2-hour fluctuation correlation with temperature, possibly due to the rubidium frequency locker. The uncorrected time difference is shown for the case of the 2.2 km fiber (divided by 1000 and offset). This variation diminishes with decreasing fiber length, as expected if the wavelength were changing. The resultant RMS variation in delay of 2850 MHz RF signal between the two arms is 19.4 fs with a 2.2 km fiber, and 8.4 fs with a 200 m fiber.

SUMMARY

In conclusion, we have demonstrated a robust RF distribution system based on common fiber and RF components, capable of low jitter operation. It is easily expandable to multiple channels, requiring only an increase in transmitter optical power and the addition of fiber optic splitters and mirrors. This system will be of use in FEL light sources and other applications requiring sub-100 fs synchronization of RF and/or lasers.

REFERENCES

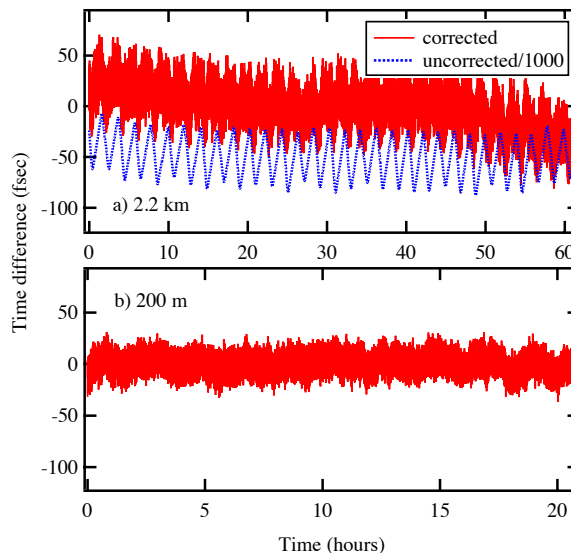[1] C. Pellegrini, in Proc. of EPAC06, Edinburgh, Scotland, 26 - 30 Jun 2006.

Figure 4: Relative drift of a 2850 MHz signal transmitted over a long and short (2 m) fiber. a) 2.2 km long fiber. The relative time difference has an RMS deviation of 19.4 fsec over 60 hours. The relative time difference (/1000) without the correction is also shown. b) A 200 m fiber has an 8.4 fsec RMS deviation over 20 hours.

[2] O. Lopez, A. Amy-Klein, C. Daussy, Ch. Chardonnet, F. Narbonneau, M. Lours, and G. Santarelli, Euro. Phys. J. D 48, 35 (2008).

[3] P. A. Williams, W. C. Swann, N. R. Newbury, J. Opt. Soc. Am. B 25 1284 (2008).

[4] H. Kiuchi, IEEE Trans. Microwave Theory and Tech., 56, 1493 (2008).

[5] D. D. Hudson, S. M. Foreman, S. T. Cundiff and J. Ye, Opt. Lett. 31, 1951 (2006).

[6] J. Kim, J. A. Cox, J. Chen, F. X. Kartner, Nature Photonics 2, 733 (2008).

[7] R. Wilcox, J. M. Byrd, L. Doolittle, G. Huang, J. Staples, Opt. Lett. 34, 3050 (2009).

[8] J. Ye, J.-L. Peng, R. Jason-Jones, K. W. Holman, J. L. Hall, D. J. Jones, S. A. Diddams, J. Kitching, S. Bize, J. C. Bergquist, L. W. Holberg, L. Robertsson, and L.S. Ma, J. Opt. Soc. Am. B 20, 1459 (2003).

[9] J. W. Staples, J. M. Byrd, L. Doolittle, G. Huang, and R. Wilcox, Proceedings of the 2008 Linear Accelerator Conference, M. Comryn, ed. (IEEE, 2008).

[10] A. Bruner, V. Mahal, I. Kiryuschev, A. Arie, M. A. Arbore, M. M. Fejer, Appl. Opt. 37, 6410 (1998).

[11] S. Masuda, A. Seki, S. Niki, Appl. Opt. 46, 4780 (2007).

[12] F. X. Kartner, H. Byun, J. Chen, F. J. Grawert, F. O. Ilday, J. Kim, and A. Winter, in Proceedings of the 2005 Particle Accelerator Conference, C. Horak, ed. (IEEE, 2005).

[13] G. Ghosh, M. Endo, and T. Iwasaki, IEEE J. of Lightwave Tech., Vol. 12, p 1338 (1994).